JOURNAL OF GEOPHYSICAL RESEARCH, VOL. 113, A12217, doi:10.1029/2008JA013366, 2008

Ultra-low-frequency waves and associated wave vectors observed in the plasma sheet boundary layer by Cluster

M. C. Broughton,[1,2] M. J. Engebretson,[2] K.-H. Glassmeier,[1] Y. Narita,[1] A. Keiling,[3] K.-H. Fornaçon,[1] G. K. Parks,[3] and H. Rème[4]

Received 2 May 2008; revised 18 July 2008; accepted 1 August 2008; published 31 December 2008.

[1] Waves in the Pc1–Pc2 frequency range (0.1–5 Hz) are studied using Cluster magnetic field data. In the plasma sheet boundary layer, Cluster observed harmonically related waves with the fundamental near the local proton cyclotron frequency (Ω_p). These waves had components both parallel and perpendicular to the local magnetic field ($\mathbf{B}_0$). Application of the wave telescope yielded the full wave vector ($\mathbf{k}$) of the waves and showed that they propagated nearly perpendicular to $\mathbf{B}_0$. Associated with the waves were two counterstreaming ion beams with a relative velocity of approximately 4000 km/s. During wave activity, the tailward streaming beam increased in energy flux, and subsequently, energy flux increased in directions perpendicular to $\mathbf{B}_0$. We suggest two possible sources for the waves: inverse Landau resonance with an accelerated electron beam and an electromagnetic ion/ion cyclotron instability. The change in the ion distribution suggests these waves could contribute to the formation of the hot protons of the central plasma sheet.

Citation: Broughton, M. C., M. J. Engebretson, K.-H. Glassmeier, Y. Narita, A. Keiling, K.-H. Fornaçon, G. K. Parks, and H. Rème (2008), Ultra-low-frequency waves and associated wave vectors observed in the plasma sheet boundary layer by Cluster, *J. Geophys. Res.*, *113*, A12217, doi:10.1029/2008JA013366.

1. Introduction

[2] The Cluster spacecraft provide new opportunities to study waves in the Pc1–Pc2 frequency range (0.1–5 Hz) generated in several regions of Earth's magnetosphere. When its four spacecraft are in the correct configuration, Cluster can measure the full wave vector ($\mathbf{k}$), which provides both the wavelength and the propagation direction of a wave. Previous wave telescope work has been used to determine dispersion relations [*Narita and Glassmeier*, 2005], propagation patterns [*Narita et al.*, 2006a], energy spectra [*Narita et al.*, 2006b] and cross-helicity [*Narita et al.*, 2007]. Using Cluster, we present measurements of $\mathbf{k}$ for waves with frequencies near the harmonics of the local proton cyclotron frequency (Ω_p).

[3] Several early studies of waves at geosynchronous orbit [see, e.g., *Russell et al.*, 1970; *Gurnett*, 1976] reported observations of harmonically related, monochromatic ultra-low-frequency waves at and often considerably above Ω_p. These waves were observed within 10 degrees of the geomagnetic equator, had stronger fluctuating magnetic components parallel to the local magnetic field ($\mathbf{B}_0$) than transverse to it, and were closely associated with ring-like distributions of protons. *Perraut et al.* [1982] presented a systematic study of harmonically related, monochromatic ULF waves above Ω_p observed by GEOS 1 and 2. These waves were observed within 10 degrees of the geomagnetic equator at L values between ~4 and ~8, propagated perpendicular to $\mathbf{B}_0$, and were closely associated with ring-like distributions of protons peaking at energies in the range $5 \leq E \leq 30$ keV. Using data from GEOS 2, *Laakso et al.* [1990] studied the wave electric field of these waves, finding that it was right-handed with the major axis of the polarization ellipse nearly parallel to both the predicted wave vector and the azimuthal direction. *McClements et al.* [1994] proposed that harmonically structured ULF waves observed near the equator were actually obliquely propagating fast Alfvén waves, which propagated in the azimuthal direction with respect to $\mathbf{B}_0$.

[4] In the magnetotail and plasma sheet boundary layer (PSBL), observations of waves near the proton gyrofrequency are numerous. *Tsurutani and Smith* [1984] and *Tsurutani et al.* [1985] reported observations of magnetosonic waves, observed when ISEE 3 was in the distant PSBL ($X_{GSE} < -220\ R_E$). These waves had rest frame frequencies from 0.3 to 2.0 Ω_p, were mainly polarized in a right-handed sense, and propagated 0 to 30 degrees away from $\mathbf{B}_0$. Highly anisotropic, tailward streaming, relatively cold ion beams occurred in near-time coincidence with these waves. As the authors pointed out, during substorms, plasma in the magnetotail can exhibit a significant pressure anisotropy, which if greater than the magnetic tension, could

[1]Institut für Geophysik und extraterrestrische Physik, Technische Universität Braunschweig, Braunschweig, Germany.
[2]Department of Physics, Augsburg College, Minneapolis, Minnesota, USA.
[3]Space Sciences Laboratory, University of California, Berkeley, California, USA.
[4]Centre d'Etude Spatiale des Rayonnements, CNRS, Toulouse, France.

0148-0227/08/2008JA013366$09.00

generate waves near Ω_p that are right-hand circularly polarized.

[5] The counterstreaming ions of the PSBL offer many possible instabilities for wave growth. *Gary and Winske* [1990] listed possible instabilities, of which we will discuss four. First, the relative drift of ions and electrons could create a field-aligned current, leading to a kink-like instability. This would generate waves with the largest growth rate parallel or antiparallel to $\mathbf{B}_0$. Second, a temperature anisotropy could provide energy for the electromagnetic ion cyclotron instability, also generating parallel and antiparallel propagating waves. The final two instabilities are the ion/ion nonresonant and right-hand resonant instabilities, both of which are caused by the relative drift of ions along $\mathbf{B}_0$.

[6] *Angelopoulos et al.* [1989] presented a linear theory for electromagnetic waves propagating parallel to $\mathbf{B}_0$ in the PSBL. The linear theory presented predicted three wave modes: waves caused by a kink-like instability generated at short wavelengths with frequencies under Ω_p; waves along the positive helicity branch of the ion cyclotron anisotropy instability; and waves along the negative helicity branch of the same instability. The latter two instabilities were predicted to generate wave both below and slightly above Ω_p. Observationally, the appearance of two fast, counterstreaming, anisotropic ion components corresponded to a significant increase in the magnetic fluctuation energy both below and above Ω_p, in full agreement with their theoretical predictions. Later observations [*Chaston et al.*, 1994] explored the relationships among electromagnetic ion cyclotron waves, decreasing plasma beta (β), and an anisotropic earthward streaming beam with a velocity below the Alfvén velocity (v_A). Further work considered the interaction between the beam anisotropy and kink-like instabilities [*Chaston et al.*, 1999a] and the dependence of waves on the ion distributions at the wave source [*Chaston et al.*, 1997, 1999b]. Using 3 months of plasma sheet passes from the Active Magnetospheric Particle Tracer Explorers/Ion Release Module satellite, *Bauer et al.* [1995] found that for frequencies between 0.03 Hz and 2 Hz, the intensity of right-handed magnetic fluctuations was approximately equal to the intensity of left-handed fluctuations. The intensity of compressional fluctuations increased with an increase in β and in the PSBL was typically smaller than the intensity of transverse fluctuations. *Bogdanov et al.* [2003] identified ion cyclotron waves in the PSBL and tail lobes during the Cassini spacecraft's Earth flyby with frequencies relatively narrowly distributed around $\omega/\Omega_p = 0.5$, a propagation angle (θ) that varied between 10 and 90 degrees with respect to $\mathbf{B}_0$, and a predominantly linear polarization.

[7] In addition to an ion cyclotron and kink-like instability, the counterstreaming beams of the PSBL could create additional instabilities due to the relative drifts of ions. *Gary and Winske* [1990] performed simulations regarding these instabilities. The authors found that when the relative velocity of the proton beams was greater than twice the Alfvén velocity, the ion/ion nonresonant instability could grow to large amplitudes. Further, when a population of dense, cool, oxygen ions was added, v_A further decreased and the ion/ion right-hand resonant case became a source of magnetic fluctuations. The two ISEE plasma sheet crossings presented by *Angelopoulos et al.* [1989] were discussed by *Elphic and Gary* [1990], who suggested the right-hand resonant instability was the likely source for the wave fluctuations observed. However, neither high magnetic field energy densities nor large densities of oxygen ions were present, leading the authors to suggest that the waves may have propagated from farther down the tail. *Neagu et al.* [2001] pointed out that ion-driven electromagnetic instabilities may contribute to the fluctuations observed in the plasma sheet. They suggested that proton/proton type instabilities would be more likely to arise in the PSBL than in the central plasma sheet itself, consistent with earlier observations, and suggested that the proton flow speed is also an important source of free energy for the magnetic fluctuations. Additionally, the ion/ion right-hand instability has been associated with streaming beams near $X_{GSE} \sim 142$ Earth radii [*Kawano et al.*, 1994] and has been identified as a possible source for large amplitude electron/ion whistler waves [*Akimoto and Winske*, 1989].

2. Instrumentation and Data Analysis

[8] The four Cluster spacecraft were launched into a polar orbit with apogee of 19.6 Earth radii (R_E) in late summer 2000 and began full operations in February 2001 [*Escoubet et al.*, 2001]. Because the Cluster orbits are fixed with respect to inertial space, they sweep through all local times every year. During August and September, the apogee of the Cluster spacecraft precessed from ~000 magnetic local time (MLT) to ~2100 MLT. The FGM instrument on each Cluster spacecraft consists of redundant triaxial fluxgate magnetic field sensors on one of the two radial booms of the spacecraft [*Balogh et al.*, 2001] and provides 3-axis magnetic field measurements at 22.416 vectors/second in its nominal mode. The CIS experiment on the Cluster spacecraft measures the full, three-dimensional ion distribution of the major magnetospheric ions (H^+, He^+, He^{++} and O^+) from thermal energies to about 40 keV/e [*Rème et al.*, 2001]. The experiment consists of two different instruments: a Composition and Distribution Function analyzer (CODIF) that gives the mass per charge composition with medium 22.5 degree angular resolution, and a Hot Ion Analyzer (HIA) which does not offer mass resolution but has a better angular resolution of 5.6 degrees.

[9] The wave telescope technique (described in detail by *Motschmann et al.* [1996] and *Glassmeier et al.* [2001]) is a generalized minimum variance analysis that determines the magnitude and direction of a wave vector. Four important parameters should be checked to ensure accurate determination of $\mathbf{k}$ by the wave telescope. First, the background field should not exhibit large gradients. Second, the spacecraft should not traverse a large distance compared to wavelength under consideration. Third, the spacecraft configuration should be close to that of a regular tetrahedron. We use a quality parameter (Q_{GM}), discussed by *vom Stein et al.* [1992], which is defined as

$$Q_{GM} = 1 + \frac{True\ Surface}{Ideal\ Surface} + \frac{True\ Volume}{Ideal\ Volume} \quad (1)$$

where the "True" volume and surface are those formed by the four spacecraft and the "Ideal" are those of a regular tetrahedron formed with the mean distance between the

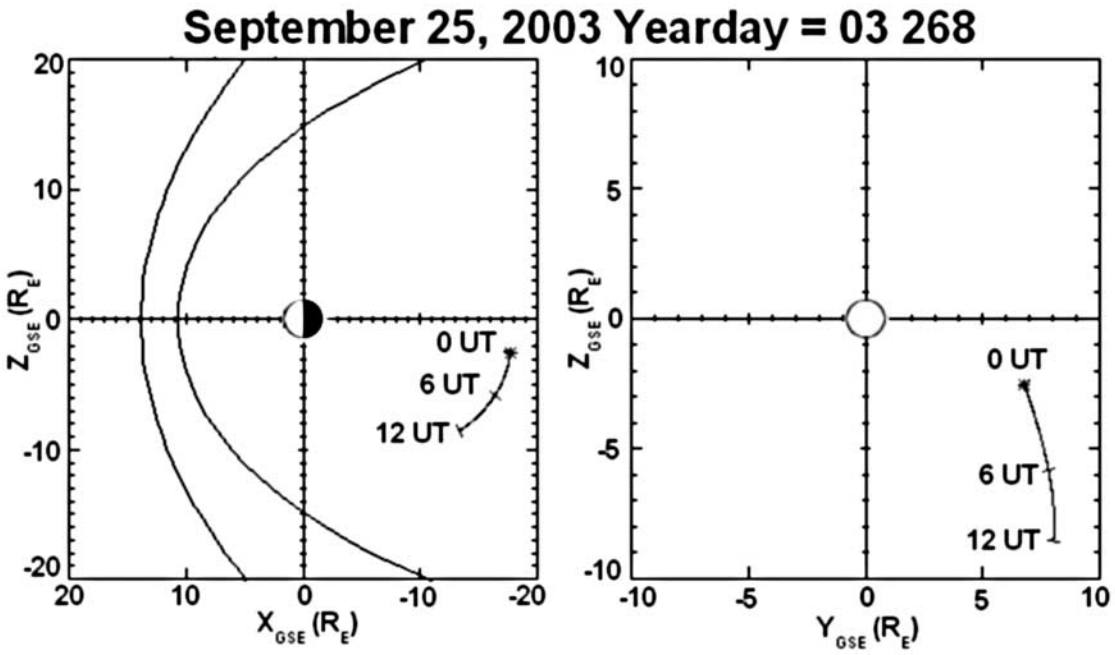

Figure 1. Position of the Cluster satellites from 0–12 UT on 25 September 2003. Plots were made using the services at the Satellite Situation Center (http://sscweb.gsfc.nasa.gov/).

spacecraft. Finally, to minimize the effects of spatial aliasing, we define a Nyquist wave number (k_{NY}) as

$$k_{NY} = k_{MAX}/2 \quad (2)$$

where k_{MAX} is the maximum distance between the sides of the parallelpiped in k-space formed by the configuration of the spacecraft.

[10] In the following sections, three different coordinate systems are used for data presentation. The first, used for spacecraft positions and wave telescope results, is the geocentric-solar-ecliptic (GSE) system with the x axis along the Earth-Sun line, the y axis pointing from dawn to dusk and the z axis extending northward from the ecliptic plane. A local field-aligned coordinate system is used for Fourier spectrograms and line plots, using a 15-min average for the mean magnetic field. In this coordinate system the z axis is in the direction of $\mathbf{B}_0$. The y axis is transverse to $\mathbf{B}_0$ and to the radius vector from the Earth to the spacecraft and is directed approximately azimuthally eastward. The x axis completes the right-handed system and is directed approximately radially outward from Earth. Since the waves Cluster observed propagated perpendicular to $\mathbf{B}_0$, a wave-vector-aligned coordinate system is used to study the polarization of the waves. In this system, z is directed along $\mathbf{k}$; x is transverse to both $\mathbf{k}$ and $\mathbf{B}_0$; y completes the right-handed system and is directed approximately along $\mathbf{B}_0$.

3. September 25, 2003

[11] Figure 1 consists of two orbit plots that show the position of Cluster from 0 to 12 UT on 25 September 2003 in units of Earth radii. The left panel, a plot of the X_{GSE} and Z_{GSE} coordinates, shows that Cluster was near apogee in the magnetotail near -18 R_E, and the right panel, a plot of Z versus Y in GSE coordinates, shows that the spacecraft were approximately 6 R_E south of the ecliptic plane.

[12] A line plot of the three components of the magnetic field in field-aligned coordinates is shown in Figure 2. The value of the mean magnetic field has been subtracted from the data. While it is not present during the entire interval, wave activity occurs near 0649 UT, 0651 UT, and 0653 UT.

[13] The two panels of Figure 3, an ion energy spectrogram and a line plot of ion density, provide information

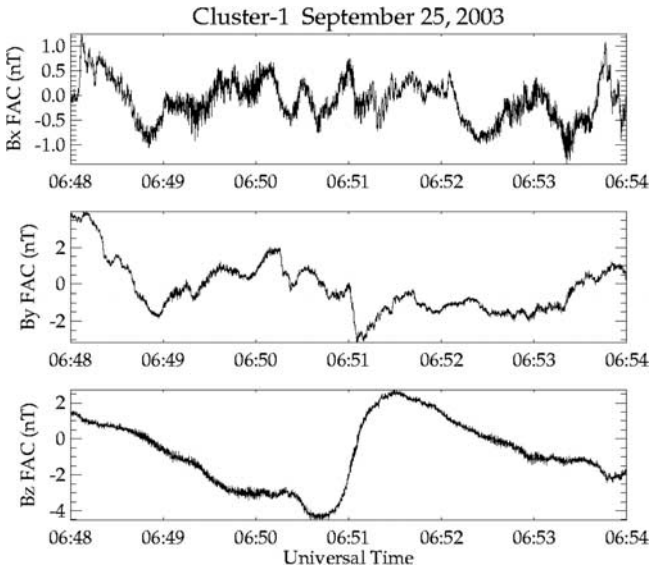

Figure 2. Line plot of the three components of the magnetic field observed by Cluster-1 on 25 September 2003. The data are in mean field-aligned coordinates. The value of the mean magnetic field has been subtracted from the field-aligned (Bz) component.

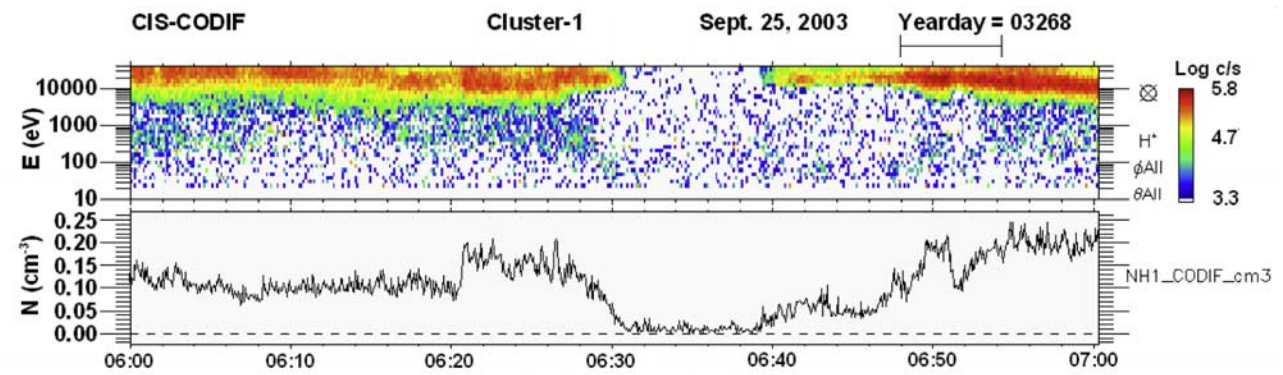

Figure 3. Ion energy spectrogram and ion density as a function of time. Data were taken from the Composition and Distribution Function analyzer (CODIF) instrument aboard Cluster-1. The bar at the top of the figure signifies the interval under consideration. Time is on the horizontal axis and is given in Universal Time. The color bar at the right represents corrected-for-detection-efficiency counts per second.

regarding the region of the magnetosphere the satellites were in. The black bar at the top of the plot is the interval during which waves were observed. The corrected-for-detection-efficiency counts per second is given by the color bar at the right side of Figure 3. Near 0640 UT, there was an increase in both ion density and in the counts per second of particles with an energy near 10000 eV. This change is consistent with the spacecraft moving from the southern tail lobes into the PSBL.

[14] A Fourier spectrogram of differenced magnetic field data in mean field-aligned coordinates is shown in Figure 4. Universal Time is along the horizontal axis of each panel with frequency in milliHertz along the vertical axis. The local proton gyrofrequency is represented by the white line in the top plot. Spectral power is indicated by the color bar on the right side of Figure 4. At approximately 0648 UT, there was an increase in spectral power in at least two frequency bands which lasted until approximately 0655 UT.

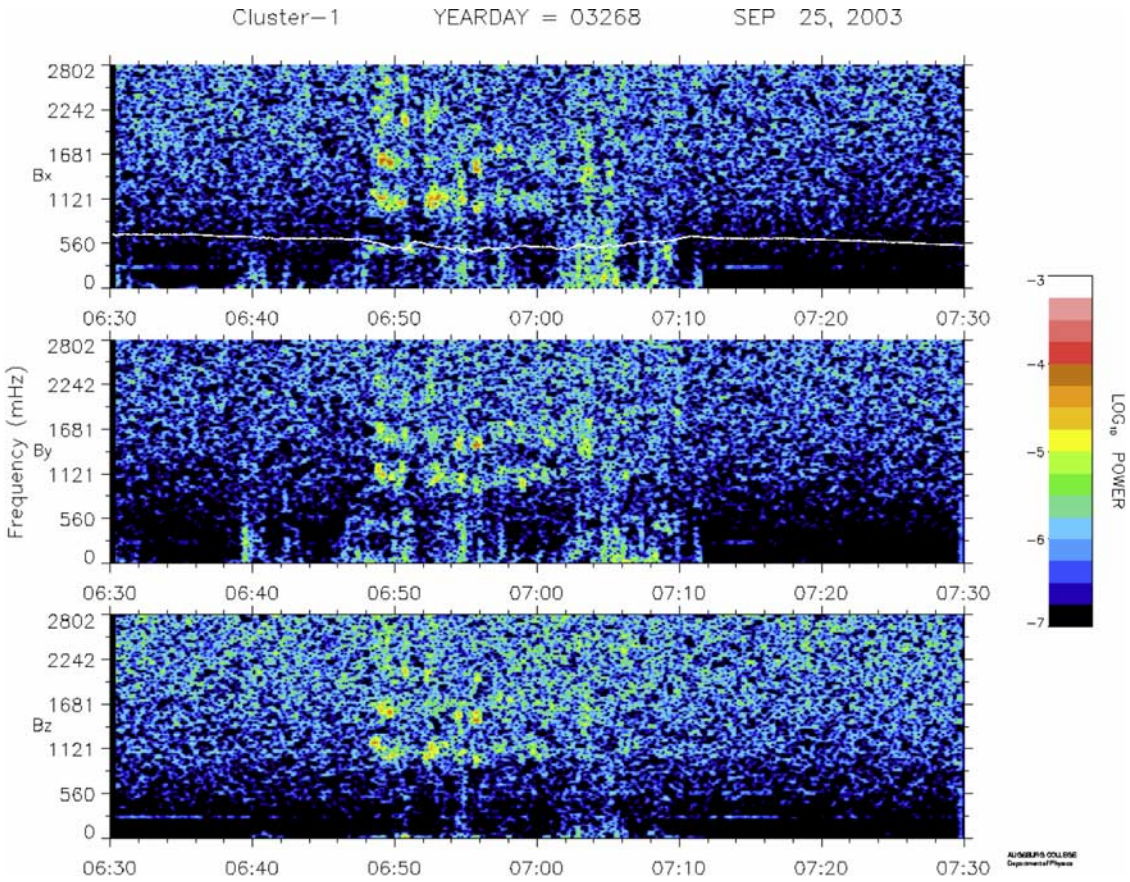

Figure 4. Time-frequency spectrogram of the three components of the magnetic field observed by Cluster-1 on 25 September 2003. The data are in field-aligned coordinates. Power is given by the color bar on the right side of the figure. The white line in the top panel is the local proton gyrofrequency.

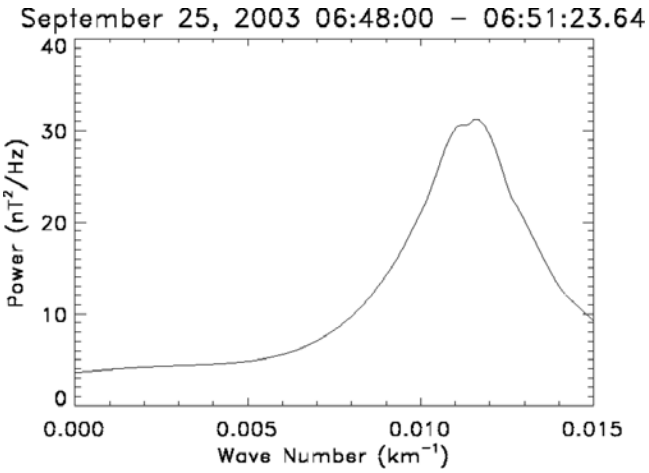

Figure 5. Plot of maximum spectral density versus wave number for the wave telescope analysis performed at 1550 mHz. During the analysis time, the Nyquist wave number was 0.01558 km^{-1}.

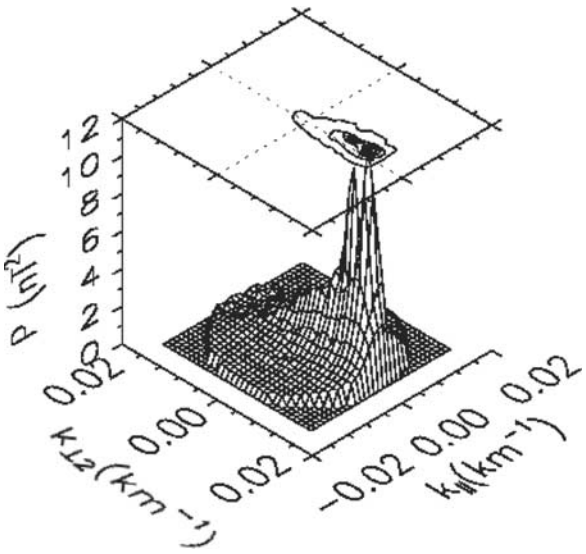

Figure 6. Plot of power as a function of the wave vectors perpendicular and parallel to $\mathbf{B}_0$.

As can be seen in Figure 4, this increase was observed in all three components of $\mathbf{B}_0$, although the fundamental tone was weak and can be seen in only the radial (Bx) and transverse (By) components. The bands of wave power correspond closely with harmonics of Ω_p.

[15] Wave telescope analysis was performed at 1550 mHz, the frequency of the third harmonic, from 0648:00 UT until 0651:23 UT. The analysis used windows of 2048 data points shifted 32 points, 76 times (4480 total points). During the analysis interval, the Nyquist wave number was 0.01558 km^{-1}, and the spacecraft configuration was nearly that of an regular tetrahedron (i.e., quality parameter of 2.98).

[16] In searching for wave power, the wave telescope technique examines concentric spherical shells in k-space, with the radius of a particular shell corresponding to a specific wave number. Each shell is scanned along all degrees of latitude and longitude for power. Figure 5 is a plot of maximum spectral density along each k-shell as a function of wave number. There is a peak at k = 0.01152 km^{-1}, corresponding to a wavelength of 545 km.

[17] To get a sense of the propagation direction, the power as a function of the wave vectors parallel and perpendicular to $\mathbf{B}_0$ is shown in Figure 6. Maximum power is quite localized, and almost none of the power is parallel to $\mathbf{B}_0$. The full wave vector in GSE coordinates was [-1.97×10^{-3} km^{-1}, 3.41×10^{-3} km^{-1}, 1.08×10^{-2} km^{-1}], and the angle between $\mathbf{k}$ and $\mathbf{B}_0$ was 82 degrees.

[18] To verify the results of the wave telescope analysis, principal axis analysis (described by *Arthur et al.* [1976]) was performed on the data using the same number and size of Fourier windows as the wave telescope analysis used. The angle between the minimum variance direction provided by the principal axis analysis and $\mathbf{k}$ was found for each satellite. The mean angle between the two was 26.5 degrees, a value that is reasonably small. Fluctuations in the magnetic field that are not attributable to the waves may be the cause of this difference.

[19] The second harmonic was stronger during a later time period, so additional wave telescope analysis was performed at 1107 mHz (the frequency of the second harmonic) from 0651:30 UT to 0655:00 UT. A total of 4608 data points were used in analysis (Fourier windows of 2048 points, shifted 32 points 80 times). The quality parameter and k_{NY} were 2.98 and 1.46×10^{-2} km^{-1} respectively. The full wave vector was [-1.02×10^{-3} km^{-1}, 5.18×10^{-3} km^{-1}, 7.04×10^{-3} km^{-1}] and formed an angle of 83 degrees with $\mathbf{B}_0$.

[20] The magnetic field data from Cluster-4 were band-pass-filtered between 0.3 Hz and 7 Hz and rotated into a wave-vector-aligned coordinate system, described above, in order to make Figure 7, a series of hodograms of the two components perpendicular to $\mathbf{k}$. The wave was clearly circularly polarized in a right-handed sense around the wave vector.

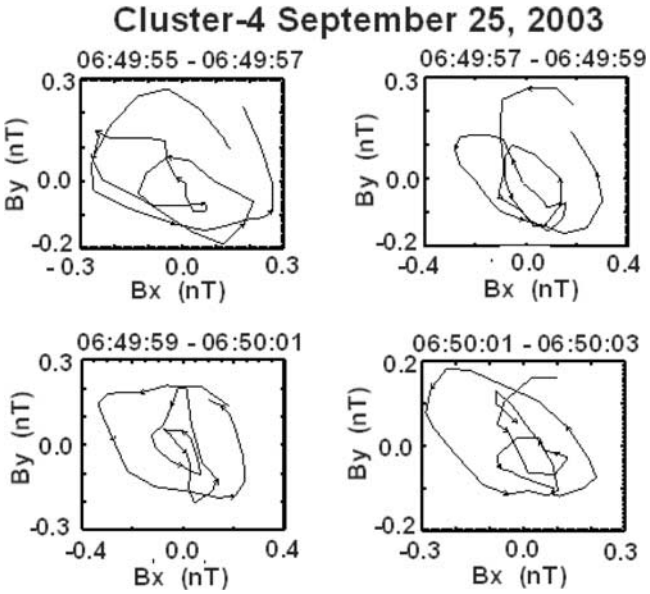

Figure 7. Plot of Bx versus By in a wave-vector-aligned coordinate system. The data have been band-pass-filtered between 0.3 Hz and 7 Hz. The wave vector is directed out of the page.

Table 1. Summary of the Multiple Harmonic Wave Events Presented in This Study[a]

Date	Time (UT)	X_{GSE}	Z_{GSE}	MLT	Ω_1/Ω_p	Amplitude of Fund (nT)	$b_\perp/b_{//}$
21 September 2002	1400–1510	−15.0	−9.2	2304	0.85	0.5	~2.0
25 September 2003	0648–0654	−16.1	−6.2	2310	0.87	0.6	~1.3
30 August 2003	0509–0513	−17.0	−7.1	0027	n/a	n/a	~1.3

[a]MLT is magnetic local time.

[21] Table 1 summarizes the properties of waves with harmonics observed by Cluster near the PSBL. All events occurred in the southern magnetotail with X_{GSE} between -15 R_E and -18 R_E and MLT near 2300. The frequency of the fundamental was within 20% of Ω_p and the amplitude of the fundamental was between 0.3 nT and 0.6 nT. Also, all events had a significant compressional component although this component was smaller than its perpendicular counterpart. For the event on 30 August 2003, the fundamental was not present.

[22] A summary of the wave vector properties for the three events for which the wave telescope could be applied is shown in Table 2. All three wave vectors were nearly perpendicular to $\mathbf{B}_0$ and had a wavelength less than 700 km. In addition, all three had the largest component in the ecliptic north direction, and two of the three wave vectors had significant components along the dawn-dusk line.

[23] In addition to their harmonic structure, perpendicular propagation, and circular polarization, these waves were associated with a change in the ion velocity distribution. Figure 8 is a series of plots of the velocity distributions before, during, and after the waves as seen by the HIA instrument aboard Cluster-1. On 25 September 2003 at 0648:09 UT, a time before waves were observed, two counterstreaming ion beams were visible in the ion distribution. Both beams had a velocity near 2000 km/s, and the earthward flowing beam had a significantly higher flux than the tailward flowing beam. The next two panels of Figure 8 show how the ion distribution evolved while the waves were observed. The flux of the tailward flowing beam increased near 0648:45 UT, approximately when Cluster-1 observed the waves, and between 0649:10 UT and 0650:22 UT, the beams became scattered into the perpendicular directions. As shown in the last panel of Figure 8, when the satellite ceased to observe the waves, the ion distribution returned to its initial state.

4. Discussion

[24] Understanding these waves could contribute to one of the outstanding questions regarding the plasma sheet boundary layer. As pointed out by multiple authors [e.g., *Gary and Winske*, 1990], a common observation of spacecraft as they move from the PSBL to the central plasma sheet is a change from two crescent-shaped distributions in velocity space to a ring-shaped distribution, to the hot protons of the central plasma sheet. Studies as early as *Forbes et al.* [1981] suggested that pitch angle scattering, a possible consequence of electromagnetic waves in the PSBL, could be a source of hot central plasma sheet ions. *Chaston et al.* [2000] discussed ion heating in the PSBL by electromagnetic waves through resonant and nonresonant processes. However, since the authors assumed $\mathbf{k} \times \mathbf{B}_0 = 0$, the extent to which these could be applicable to the waves observed by Cluster is unclear.

[25] With knowledge of **k,** ω, and the ion distribution, one can test for both proton cyclotron and Landau resonances. Proton cyclotron resonance can be tested with the following equation:

$$\omega - k_B v_B \pm m\Omega_p = 0,\ m = 1, 2, 3, \ldots, \quad (3)$$

where v_B and k_B and are ion beam velocity and the component of **k** parallel to v_B respectively. Using the results of the wave telescope, we compared the observed beam velocities with those needed to satisfy the above equation. For the observed third harmonic along the negative branch for m = 2, the cyclotron resonance condition was met when v_B = 2027 km/s, a value close to the ion beam speeds observed by Cluster. For the second harmonic to satisfy the resonance condition, the values of v_B were more than 10% away from those observed. With the observed values of ω and **k**, the ion beam speeds for Landau resonance were a factor of three larger than observed speeds.

[26] In addition to scattering by electromagnetic waves, other explanations exist regarding the formation of the ion distributions in the PSBL. For example, by using a model with quasi-steady reconnection, a velocity filter effect, conservation of energy, and conservation of magnetic moment (see *Onsager et al.* [1990, 1991] for further details), many of the observed features of the ion distribution in the PSBL have been reproduced. Since neither occurrence frequency nor the extent to which these waves scatter ions is currently known, the waves in this study can only be suggested as one possible scattering mechanism in the PSBL.

[27] Even though the frequency, polarization, and full wave vector should be enough to distinguish the wave mode, the polarization of these waves presents a problem when making comparisons with the predicted wave modes. *Stix* [1992] discussed the possible wave modes for propagation perpendicular to $\mathbf{B}_0$ close to harmonics of Ω_p; however, none of them had a circular polarization in the plane parallel $\mathbf{B}_0$. In the cold plasma limit, two of the four

Table 2. Summary of the Wave Vector Properties Measured by the Wave Telescope

Date	Frequency (mHz)	λ (km)	k_X (km^{-1})	k_Y (km^{-1})	k_Z (km^{-1})	θ (°)
25 September 2003	1550	551	-1.94×10^{-3}	3.34×10^{-3}	1.07×10^{-2}	82
25 September 2003	1107	684	-1.02×10^{-3}	5.18×10^{-3}	7.04×10^{-3}	83
30 August 2003	1676	582	-2.61×10^{-3}	6.45×10^{-3}	8.30×10^{-3}	86

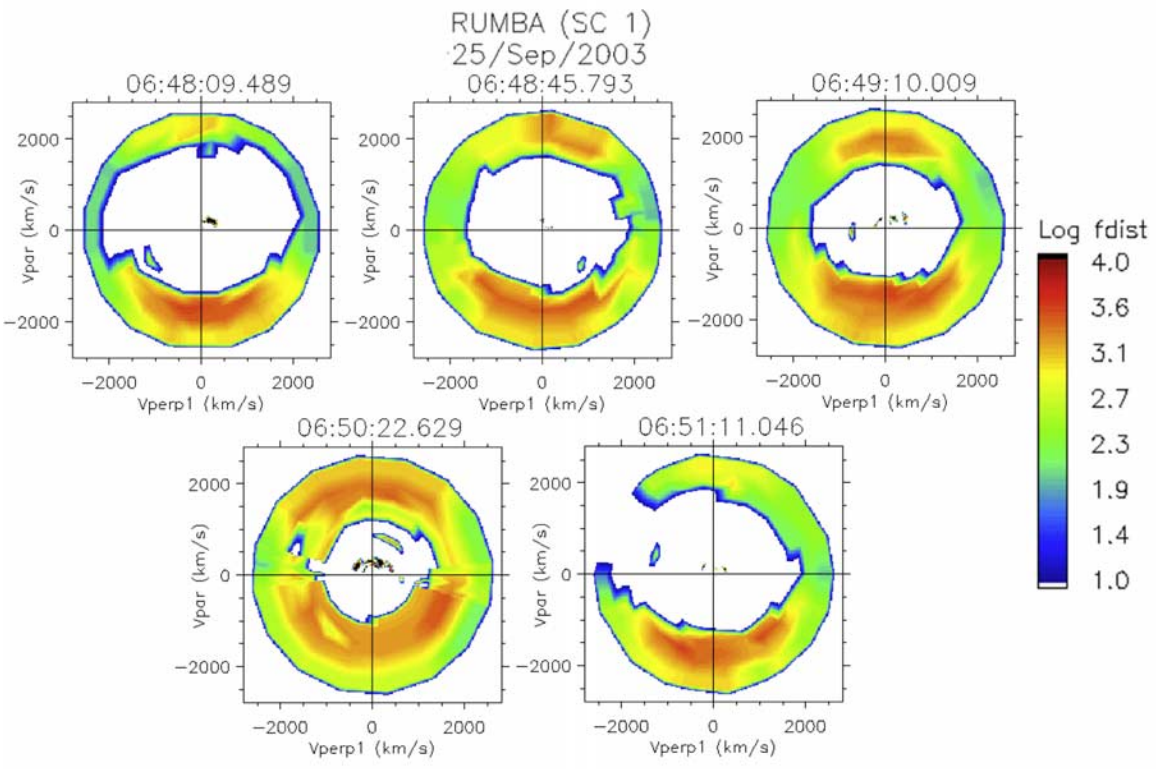

Figure 8. A series of ion velocity distributions parallel and perpendicular to the local magnetic field observed by the HIA instrument on Cluster-1 on 25 September 2003. The phase space density is indicated by the color bar at the right.

modes discussed reduced to the ordinary mode, which is linearly polarized. Of the two remaining wave modes, both of which reduced to the extraordinary mode in the cold plasma approximation, the electric field lay entirely in the plane perpendicular to $\mathbf{B}_0$.

[28] The harmonics of Ω_p and perpendicular propagation are similar to the ion Bernstein mode. Although that mode is traditionally an electrostatic mode, there have been observations of electromagnetic Bernstein modes. *Chaston et al.* [2002] identified the neutralized Bernstein mode in observations from Fast Auroral Snapshot spacecraft observations of electromagnetic waves at harmonics of Ω_p in the auroral oval and subsequent modeling. In the model presented by the authors, the waves with the strongest growth rates occurred just below harmonics of Ω_p with a $\mathbf{k}$ nearly perpendicular to $\mathbf{B}_0$. Of the two wave modes the authors identified, a neutralized ion Bernstein mode and a pure electrostatic ion Bernstein mode, the former had the higher growth rate. Wave growth was caused by inverse Landau resonance with an electron beam. Although the electrons were identified as the primary source of wave growth, the authors pointed out that ions could also play a role. In terms of ion heating, since the waves were near Ω_p, either a resonant or a nonresonant interaction between the ions and the waves could scatter the ion beam. Both of these mechanisms were discussed by *Chaston et al.* [2002].

[29] While this scenario does offer explanations for the harmonic structure, propagation direction, and ion heating, it does not explain the wave polarization of the waves observed by Cluster. Also, looking at Figure 8, it seems that only the tailward flowing beam was affected by the presence of the waves. Most significantly, we do not yet have direct observation from Cluster of either the electron beam that would excite the waves or the potential needed to accelerate that beam. Electron beams are commonly observed in the PSBL, and future work could see if there is a correlation between the observation of electron beams and the appearance of waves.

[30] The electromagnetic ion/ion cyclotron instability (EMIIC), the second possible source of the waves, is described by *Winske and Omidi* [1992] with linear theory and hybrid simulations. The instability is an extension of the nonresonant case of the electrostatic ion cyclotron instability reported by *Miura et al.* [1983]. A coupling between a slow wave on the ion beam and the cyclotron mode of the background ions is the instability that drives the waves. *Winske and Omidi* [1992] extended this instability in a plasma with finite plasma beta values ($\beta < 0.1$). Neither of the studies showed fluctuations of the magnetic field at harmonics of Ω_p, but some of the electrostatic waves in the simulations [*Miura et al.*, 1983] occurred at harmonics of Ω_p. As the electromagnetic waves described by *Winske and Omidi* [1992] propagate at angles nearly perpendicular to $\mathbf{B}_0$, the electromagnetic instability is similar to the electrostatic instability, an instability that could produce waves near proton cyclotron harmonics. Additionally, the authors did identify ion heating as a consequence of waves caused by the EMIIC instability. The Cluster observations did occur in plasma with β greater than the values considered by the authors, but it could be the source the electromagnetic waves.

[31] Since Cluster was in a region with a $\beta > 0.1$, additional ion/ion instabilities should be considered. *Gary* [1991] provided a review of electromagnetic ion/ion instabilities. The ion/ion right-hand resonant and ion/ion nonresonant instabilities could be significant. However, the propagation angle of the waves observed by Cluster differed significantly from those presented in previous models and observations of waves. *Gary and Winske* [1990] pointed out that both instabilities have maximum growth parallel to $\mathbf{B}_0$. *Elphic and Gary* [1990] suggested that waves observed by ISEE during two crossings of the PSBL were caused by the right-hand resonant instability. The authors admitted that a dense population of cold ionospheric oxygen was needed, leading them to propose that the waves were generated farther down in the tail. Since our observations showed no relatively dense ionospheric oxygen and propagation from further down the tail is unlikely, they were probably not caused by the right-hand resonant instability. Additional instabilities related to beam anisotropies or a kink-like instability could be the source, but previous observations and modeling [e.g., *Chaston et al.*, 1999a, 1999b] indicated that waves generated by these instabilities would occur under Ω_p and would propagate predominantly along $\mathbf{B}_0$.

5. Conclusions

[32] We have performed a study of waves occurring at multiple harmonics of Ω_p observed by Cluster in the PSBL. Because of favorable spacecraft configuration, we were able to use the wave telescope technique to measure the full **k** vector, which revealed nearly perpendicular propagation. Additional analysis of CIS data showed that the waves were associated with the perpendicular heating of tailward streaming ions. We suggest that these waves were caused by either (1) inverse Landau resonance with an accelerated electron beam described by *Chaston et al.* [2002] or (2) the electromagnetic ion/ion instability caused by coupling between a slow wave on the ion beam and the background ions described by *Winske and Omidi* [1992].

[33] Outstanding questions remain with the waves. Neither scenario fully explains all of the qualities of the waves observed by Cluster. Also, the exact mechanism of ion heating is unclear. Further work should be done to resolve the ambiguities, and a larger study of the occurrence of these waves could show if and to what extent these waves contribute to the scattering of ions into the hot isotropic distribution of the central plasma sheet.

[34] **Acknowledgments.** The work of MCB and MJE on Cluster was supported by grants from the German Fulbright Commission. Work at Augsburg College was supported by NSF grants ATM-0305483 and ANT-0538379 and the Minnesota Space Grant College Consortium. The work at the University of California, Berkeley, was supported by NASA grant NNG05GL27G-06/08. The work at the Technical University of Braunschweig was supported by German Bundesministerium für Wirtschaft und Technologie and the Deutsches Zentrum für Luft- und Raumfahrt under contract 50OC0103.

[35] Wolfgang Baumjohann thanks Rudolf Treumann and another reviewer for their assistance in evaluating this paper.

References

Akimoto, K., and D. Winske (1989), Nonlinear generation of whistler waves by an ion beam, *J. Geophys. Res.*, *94*, 17,259–17,265, doi:10.1029/JA094iA12p17259.

Angelopoulos, V., R. C. Elphic, S. P. Gary, and C. Y. Huang (1989), Electromagnetic instabilities in the plasma sheet boundary layer, *J. Geophys. Res.*, *94*, 15,373–15,383, doi:10.1029/JA094iA11p15373.

Arthur, C. W., R. L. McPherron, and J. D. Means (1976), A comparative study of three techniques for using the spectral matrix in wave analysis, *Radio Sci.*, *11*, 833–845.

Balogh, A., et al. (2001), The Cluster magnetic field investigation: Overview of in-flight performance and initial results, *Ann. Geophys.*, *19*, 1207–1217.

Bauer, T. M., W. Baumjohann, R. A. Treumann, N. Sckopke, and H. Lühr (1995), Low-frequency waves in the near-Earth plasma sheet, *J. Geophys. Res.*, *100*, 9605–9618, doi:10.1029/95JA00136.

Bogdanov, A. T., K.-H. Glassmeier, G. Musmann, M. K. Dougherty, S. Kellock, P. Slootweg, and B. Tsurutani (2003), Ion cyclotron waves in the Earth's magnetotail during CASSINI's Earth swing-by, *Ann. Geophys.*, *21*, 2043–2057.

Chaston, C. C., Y. D. Hu, B. J. Fraser, R. C. Elphic, and C. Y. Huang (1994), Electromagnetic ion cyclotron waves observed in the near Earth plasma sheet boundary layer, *J. Geomagn. Geoelectr.*, *46*, 987–995.

Chaston, C., Y. Hu, and B. Fraser (1997), Non-Maxwellian particle distributions and electromagnetic ion cyclotron instabilities in the near-Earth magnetotail, *Geophys. Res. Lett.*, *24*(22), 2913–2916.

Chaston, C. C., Y. D. Hu, and B. J. Fraser (1999a), Quasilinear evolution of the ion cyclotron beam-anisotropy instability in a current carrying plasma, *Phys. Plasmas*, *6*, 2588–2597, doi:10.1063/1.873530.

Chaston, C. C., Y. D. Hu, and B. J. Fraser (1999b), Electromagnetic ion cyclotron waves in the near-Earth magnetotail, *J. Geophys. Res.*, *104*, 6953–6972, doi:10.1029/1998JA900139.

Chaston, C. C., Y. D. Hu, and B. J. Fraser (2000), Quasi-linear ion cyclotron heating in the near-Earth magnetotail, *J. Geophys. Res.*, *105*, 5507–5516, doi:10.1029/1999JA900466.

Chaston, C. C., J. W. Bonnell, J. P. McFadden, R. E. Ergun, and C. W. Carlson (2002), Electromagnetic ion cyclotron waves at proton cyclotron harmonics, *J. Geophys. Res.*, *107*(A11), 1351, doi:10.1029/2001JA900141.

Elphic, R. C., and S. P. Gary (1990), ISEE observations of low frequency waves and ion distribution function evolution in the plasma sheet boundary layer, *Geophys. Res. Lett.*, *17*, 2023–2026, doi:10.1029/GL017i011p02023.

Escoubet, C. P., M. Fehringer, and M. Goldstein (2001), The Cluster mission, *Ann. Geophys.*, *19*, 1197–1200.

Forbes, T. G., E. W. Holmes, S. J. Barne, J. R. Ashbridge, G. Paschmann, N. Sckopke, and C. T. Russell (1981), Evidence for the tailward retreat of a magnetic neutral line in the magnetotail during substorm recovery, *Geophys. Res. Lett.*, *8*, 261–264, doi:10.1029/GL008i003p00261.

Gary, S. P. (1991), Electromagnetic ion/ion instabilities and their consequences in space plasmas: A review, *Space Sci. Rev.*, *56*, 373–415, doi:10.1007/BF00196632.

Gary, S. P., and D. Winske (1990), Computer simulations of electromagnetic instabilities in the plasma sheet boundary layer, *J. Geophys. Res.*, *95*, 8085–8094, doi:10.1029/JA095iA06p08085.

Glassmeier, K.-H., et al. (2001), Cluster as wave telescope: First results from the fluxgate magnetometer, *Ann. Geophys.*, *19*, 1439–1477.

Gurnett, D. A. (1976), Plasma wave interactions with energetic ions near the magnetic equator, *J. Geophys. Res.*, *81*, 2765–2770, doi:10.1029/JA081i016p02765.

Kawano, H., M. Fujimoto, T. Mukai, T. Yamamoto, T. Terasawa, Y. Saito, S. Machida, S. Kokubun, and A. Nishida (1994), Right-handed ion/ion resonant instability in the plasma sheet boundary layer: GEOTAIL observation in the distant tail, *Geophys. Res. Lett.*, *21*, 2887–2890, doi:10.1029/94GL02106.

Laakso, H., H. Junginger, A. Roux, R. Schmidt, and C. de Villedary (1990), Magnetosonic waves above fc(H+) at geostationary orbit: GEOS 2 results, *J. Geophys. Res.*, *95*, 10,609–10,621, doi:10.1029/JA095iA07p10609.

McClements, K. G., R. O. Dendy, and C. N. Lashmore-Davis (1994), A model for the generation of obliquely propagating ULF waves near the magnetic equator, *J. Geophys. Res.*, *99*, 23,685–23,693, doi:10.1029/94JA01979.

Miura, A., H. Okuda, and M. Ashour-Abdalla (1983), Ion-beam-driven electrostatic ion cyclotron instabilities, *Geophys. Res. Lett.*, *10*, 353–356, doi:10.1029/GL010i004p00353.

Motschmann, U., T. Woodward, K.-H. Glassmeier, D. J. Southwood, and J. Pinçon (1996), Wavelength and direction filtering by magnetic measurements at satellite arrays: Generalized minimum variance analysis, *J. Geophys. Res.*, *101*, 4961–4966, doi:10.1029/95JA03471.

Narita, Y., and K.-H. Glassmeier (2005), Dispersion analysis of low-frequency waves through the terrestrial bow shock, *J. Geophys. Res.*, *110*, A12215, doi:10.1029/2005JA011256.

Narita, Y., K.-H. Glassmeier, K.-H. Fornaçon, I. Richter, S. Schäfer, U. Motschmann, I. Dandouras, H. Rème, and E. Georgescu (2006a),

Low-frequency wave characteristics in the upstream and downstream regime of the terrestrial bow shock, *J. Geophys. Res.*, *111*, A01203, doi:10.1029/2005JA011231.

Narita, Y., K.-H. Glassmeier, and R. A. Treumann (2006b), Wave-number spectra and intermittency in the terrestrial foreshock region, *Phys. Rev. Lett.*, *97*, doi:10.1103/PhysRevLett.97.191101.

Narita, Y., K.-H. Glassmeier, M. Fränz, Y. Nariyuki, and T. Hada (2007), Observations of linear and nonlinear processes in the foreshock wave evolution, *Nonlinear Process. Geophys.*, *14*, 361–371.

Neagu, E., S. P. Gary, J. E. Borovsky, W. Baumjohann, and R. A. Treumann (2001), Constraints on magnetic fluctuation energies in the plasma sheet, *Geophys. Res. Lett.*, *28*, 919–922, doi:10.1029/2000GL012384.

Onsager, T. G., M. F. Thomsen, J. T. Gosling, and S. J. Bame (1990), Electron distributions in the plasma sheet boundary layer: Time-of-flight effects, *Geophys. Res. Lett.*, *17*, 1837–1840, doi:10.1029/GL017i011p01837.

Onsager, T. G., M. F. Thomsen, R. C. Elphic, and J. T. Gosling (1991), Model of electron and ion distributions in the plasma sheet boundary layer, *J. Geophys. Res.*, *96*, 20,999–21,011, doi:10.1029/91JA01983.

Perraut, S., A. Roux, P. Robert, R. Gendrin, J. A. Sauvaud, J. M. Bosqued, G. Kremser, and A. Korth (1982), A systematic study of ULF waves above F_H+ from GEOS 1 and 2 measurements and their relationships with proton ring distributions, *J. Geophys. Res.*, *87*, 6219–6236, doi:10.1029/JA087iA08p06219.

Rème, H., et al. (2001), First multispacecraft ion measurements in and near the Earth's magnetosphere with the identical Cluster ion spectrometry (CIS) experiment, *Ann. Geophys.*, *19*, 1303–1354.

Russell, C. T., R. E. Holzer, and E. J. Smith (1970), OGO 3 observations of ELF noise in the magnetosphere: 2. The nature of the equatorial noise, *J. Geophys. Res.*, *75*, 755–768, doi:10.1029/JA075i004p00755.

Stix, T. H. (1992), *Waves in Plasmas*, pp. 276–285, Springer, New York.

Tsurutani, B. T., and E. J. Smith (1984), Magnetosonic waves adjacent to the plasma sheet in the distant magnetotail: ISEE-3, *Geophys. Res. Lett.*, *11*, 331–334, doi:10.1029/GL011i004p00331.

Tsurutani, B. T., I. G. Richardson, R. M. Thorne, W. Butler, E. J. Smith, S. W. H. Cowley, S. P. Gary, S.-I. Akasofu, and R. D. Zwickl (1985), Observations of the right-hand resonant ion beam instability in the distant plasma sheet boundary layer, *J. Geophys. Res.*, *90*, 12,159–12,172, doi:10.1029/JA090iA12p12159.

vom Stein, R., K.-H. Glassmeier, and M. Dunlop (1992), A configuration parameter for the Cluster satellites, *Tech. Rep. 2/92*, pp. 6–8, Inst. Geophys., Technical Univ. of Braunschweig, Germany.

Winske, D., and N. Omidi (1992), Electromagnetic ion/ion cyclotron instability: Theory and simulations, *J. Geophys. Res.*, *97*, 14,779–14,799, doi:10.1029/92JA00902.

M. C. Broughton, K.-H. Fornaçon, K.-H. Glassmeier, and Y. Narita, Institut für Geophysik und extraterrestrische Physik, Technische Universität Braunschweig, Mendelssohnstrasse 3, D-38106, Braunschweig, Germany. (mattbroughton0@gmail.com)

M. J. Engebretson, Department of Physics, Augsburg College, 2211 Riverside Avenue, Minneapolis, MN 55454-1350, USA.

A. Keiling and G. K. Parks, Space Sciences Laboratory, University of California, 7 Gauss Way, 7450, Berkeley, CA 94720-7450, USA.

H. Rème, CESR, CNRS, BP4346, F-31028, Toulouse CEDEX 4, France.